10-2015

Photocatalytic Concrete Pavements: Laboratory Investigation of NO Oxidation Rate Under Varied Environmental Conditions

Joel K. Sikkema
Dordt College, joel.sikkema@dordt.edu

Sae-Kee Ong
Iowa State University

James E. Alleman
Iowa State University

Photocatalytic Concrete Pavements: Laboratory Investigation of NO Oxidation Rate Under Varied Environmental Conditions

Abstract
Concrete pavements containing TiO_2 can be used for air pollution control by oxidizing NO_X under UV-bearing sunlight. This study employed a bench-scale photoreactor to estimate NO oxidation rates for varied environmental conditions. Rates correlated positively with NO inlet concentration and irradiance and negatively with relative humidity. No correlation occurred with flow rate. A decrease in slab moisture (previously unstudied) positively correlated with NO oxidation rate at 0–2% loss of saturated mass, but negatively correlated at losses greater that 2%. Although prior researchers deemed temperature insignificant, data indicated a positive correlation. Overall, rates ranged from 9.8–64 $nmol \cdot m^{-2} \cdot s^{-1}$.

Keywords
photocatalytic pavement, air pollution mitigation, nitrogen oxides, titanium dioxide, photoreactor bench-scale study

Disciplines
Construction Engineering and Management

Photocatalytic concrete pavements: Laboratory investigation of NO oxidation rate under varied environmental conditions

Abstract

Concrete pavements containing TiO_2 can be used for air pollution control by oxidizing NO_X under UV-bearing sunlight. This study employed a bench-scale photoreactor to estimate NO oxidation rates for varied environmental conditions. Rates correlated positively with NO inlet concentration and irradiance and negatively with relative humidity. No correlation occurred with flow rate. A decrease in slab moisture (previously unstudied) positively correlated with NO oxidation rate at 0–2% loss of saturated mass, but negatively correlated at losses greater that 2%. Although prior researchers deemed temperature insignificant, data indicated a positive correlation. Overall, rates ranged from 9.8–64 $nmol \cdot m^{-2} \cdot s^{-1}$.

Keywords

Photocatalytic pavement; air pollution mitigation; nitrogen oxides; titanium dioxide; photoreactor bench-scale study

1. Introduction

Within the United States, an estimated 48 million people live within 90 m of a four-lane (or larger) highway, railroad, or airport (Primary National Ambient Air Quality Standards for Nitrogen Dioxide: Proposed Rule, 2009). This population segment is susceptible to negative health effects associated with NO_2 exposure (Brauer et al., 2002; Brunekreef et al., 1997; Finkelstein et al., 2004; Garshick et al., 2003; Kim et al., 2004). Nitrogen dioxide (NO_2), a motor vehicle air pollutant, is regulated by the United States Environmental Protection Agency (USEPA). The agency's justification for this regulation has recently been confirmed with evidence from multiple epidemiologic studies associating short-term NO_2 exposure and adverse respiratory symptoms, particularly in children and those affected with asthma (USEPA, 2008b).

NO_2 falls within a group of highly reactive oxides of nitrogen commonly known as NO_X. Nitric oxide (NO) accounts for 95% of NO_X emissions (USEPA, 2001). This pollutant is freely oxidized to NO_2 in the atmosphere; hence, the efforts to abate NO_2 pollution target NO emissions. In fact, due to the high reactivity of the various NO_X species, USEPA assumes all NO_X in emissions estimates to be in the form of NO_2 (USEPA, 2001). USEPA employs various mechanisms in an effort to minimize NO_X exposure (e.g., improvements in public transportation, establishment of lanes for high occupancy vehicles, facilitating non-automobile travel, and promulgation of tailpipe NO_X emissions standards) (Clean Air Act, 2008; USEPA, 2007). NO_X mitigation strategies are not exempt from the law of diminishing marginal returns; therefore, in addition to efficiently applying conventional mechanisms, novel technologies should be considered. These technologies may yield higher levels of pollution reduction per dollar spent. Photocatalytic pavements represent one of these novel approaches. When exposed to sunlight and in the presence of a low concentration of water molecules, titanium dioxide (TiO_2) contained within these pavements generates hydroxyl radicals ($^{\bullet}OH$), a powerful oxidizing agent. These radicals promote the oxidation of a variety of organic and inorganic pollutants. Notably, the photocatalytic property of these pavements results in oxidation of NO_X to NO_3^- (Figure 1).

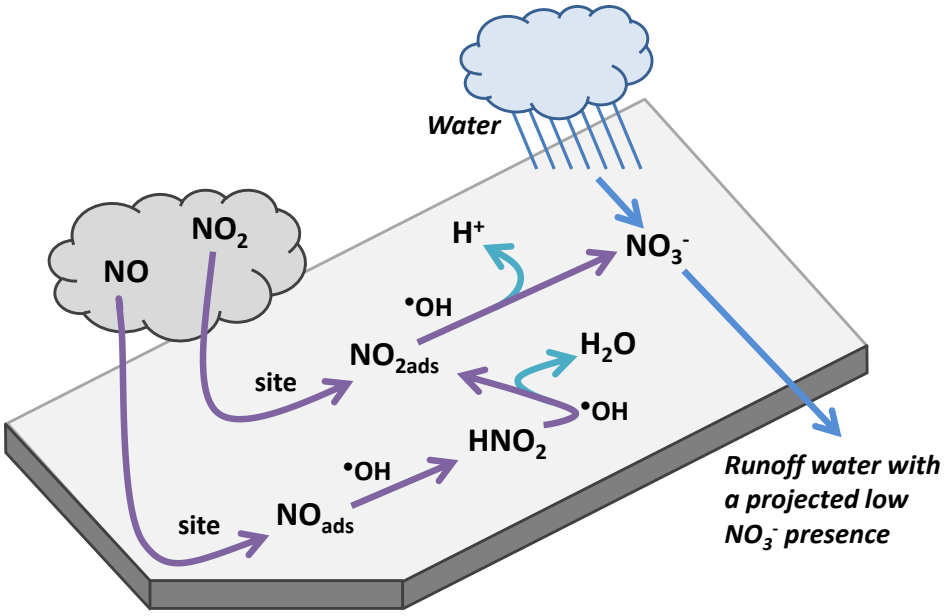

Figure 1. Photocatalytic oxidation of NO and NO_2 by pavement containing TiO_2 (partially adapted from Ballari et al., 2011).

Employment of these pavements as a mechanism to minimize the ambient concentration of NO in a targeted area will require an extensive development of what is known about NO oxidation rates under varied environmental conditions. In an effort to provide this new knowledge, various researchers have published accounts of laboratory studies that evaluated photocatalytic pavement specimens within a photoreactor, an experimental apparatus that allows for the control of various environmental conditions (Dylla et al., 2010; Hüsken et al., 2009; Murata & Tobinai, 2002). Independent environmental variables investigated have included NO concentration, irradiance, test gas flow rate, and relative humidity. Although material variables, such as TiO2 concentration and type, will also play a role, environmental variable results presented to date have not brought about a consensus in terms of the range in NO oxidation rates that can be expected. Murata et al. (2000), Hüsken et al. (2009), and Ballari et al. (2011) each suggest that NO oxidation rates positively correlate with NO concentration in situations when the photocatalytic surface was not saturated by NO; however, for tests conducted at the same environmental

conditions (1.0 ppmv, 10 $W \cdot m^{-2}$, 3 $L \cdot min^{-1}$, 50% RH) the range in oxidation rates was wide (38–84 $nmol \cdot m^{-2} \cdot s^{-1}$). Similarly, publications have noted a positive correlation between irradiance and oxidation rate, but at 10 $W \cdot m^{-2}$ calculated oxidation rates were 87 $nmol \cdot m^{-2} \cdot s^{-1}$ for Murata et al. (2000) and 24 $nmol \cdot m^{-2} \cdot s^{-1}$ for Hüsken et al. (2009). Both Murata et al. (2000) and Hüsken et al. (2009) observed a negative correlation between relative humidity and oxidation rate; however, at 50% relative humidity oxidation rates differed by 22 $nmol \cdot m^{-2} \cdot s^{-1}$. These prior studies have assumed that water vapor from the atmosphere serves as both the source of $^{\bullet}OH$ required for photocatalytic oxidation and the material which adsorbs on the surface and blinds photocatalytically active sites. Yet, given the porous nature of cementitious mixtures, water contained within a pavement could also serve as a $^{\bullet}OH$ source and blinding material. At the time of placement, these pores can become filled with water. As hydration occurs and pores become filled with air, water that is available as a $^{\bullet}OH$ source and blinding material decreases. Therefore, a decrease in moisture contained in the slab could lead to a either an increase or decrease in the NO oxidation rate of the slab; however, no lab investigation has tested this hypothesis. Hüsken et al. (2009) observed a positive correlation between percent NO removal (as opposed to NO oxidation rate) and flow rate (slope of a linear fit was less than -10). This finding was also reported in Ballari et al. (2010), however in this case slope was only slightly less than -1. Finally, a review of the fundamentals of heterogeneous catalysis indicates that, due to the fact that reactant adsorption is dependent on temperature, oxidation rate appears to be correlated with temperature (Herrmann, 2010). However, literature pertaining to photocatalytic pavements is both vague and contradictory in terms of the relationship between slab temperature and NO oxidation, with one source asserting that oxidation rate increases with an increase in temperature (Beeldens et al., 2011) and another reporting a decrease in oxidation rate with increased temperature (Chen & Chu, 2011).

Consequently, this study employed TX Active mortar slabs and a photoreactor to evaluate the change in NO oxidation rate that occurs with changes in NO concentration, irradiance, test gas flow rate, relative

humidity, decrease in slab moisture, or temperature. In instances when published photocatalytic pavement data existed, the data collected in this study was compared with data published by other researchers in order to draw conclusions in regards to the range of NO oxidation rates that could be expected and the variation that occurs between specimens.

2. Materials and Methods

2.1. Photocatalytic Mortar Slab Preparation and Cleaning

Three photocatalytic mortar slabs were used to evaluate this study's objectives. These slabs measured 152 mm (6 in) × 152 mm (6 in) × 25 mm (1 in). For this study, the researchers used a commercially-available cement that contains TiO_2 (TX Active, Essroc Italcementi Group, Nazareth, PA). Although, the TiO_2 content in this cement was not provided by the manufacturer, within patents governing photocatalytic cements, TiO_2 content ranges from 2–10% by mass (Paz, 2010). The proportions of the cement (TX Active or Type I), water, and fine aggregate (ASTM C778 standard sand, U.S. Silica Co., Frederick, MD) were recorded as 624 $kg \cdot m^{-3}$ (1052 $lb \cdot yd^{-3}$), 262 $kg \cdot m^{-3}$ (442 $lb \cdot yd^{-3}$), and 1412 $kg \cdot m^{-3}$ (2380 $lb \cdot yd^{-3}$) respectively. Given the cement proportion and the range in TiO_2 cement content above, estimated TiO_2 content of the mortar was 12.5–62.4 $kg \cdot m^{-3}$. Given the small volume of the slabs constructed, the mix did not include coarse aggregate. Except for the coarse aggregate, the relative proportions of materials used to manufacture the laboratory mortar slabs were similar to that of a pavement section placed at a field site, which will be evaluated in future research efforts *(citation removed to ensure blind review)*. Particular care was taken to use the same water-to-cement ratio for both lab and field mixtures. During the placement process, a paste of water and photocatalytic cement coats aggregates and when hardened forms the surface that is exposed to pollutants. To manufacture the slabs, a two-lift procedure was used with equal volumes of a Type I cement bottom lift followed by a TX Active photocatalytic cement top lift. A possibility exists that excess vibration and surface finishing could draw water to the surface, thereby reducing the TiO_2 concentration. To minimize this possibility the material was consolidated by tapping the sides of the form

with a mallet and leveled with use of a screed. Following placement, a damp cloth and plastic sheet were laid over the slab surface for a 24-h curing period. Following this initial curing period, the slabs were removed from the forms and placed in a 100% relative humidity room for the duration of a 14-d curing period.

Prior to evaluating NO oxidation rates (described in Section 2.3), slabs were cleaned by immersion in water (Type I reagent grade) for 2 h and oven-dried at 60°C (140°F) for 20 h. This procedure was similar to that specified by the International Organization for Standardization (ISO) standard 22197-1:2007(E); this standard governs evaluation of NO removal by photocatalytic materials (ISO, 2007).

2.2. Experimental Apparatus

A flow-through poly(methyl methacrylate) (PMMA, i.e., plexiglass) photoreactor served as the primary component of the experimental apparatus. Figure 2 provides a schematic of the photoreactor, along with the NO test gas supply system, UV-A light source, and NO/NO_X monitor. The international standard, ISO 22197-1:2007(E), provided information on the construction and operation of the setup (ISO, 2007). The test gas supplied to the photoreactor was a mixture of breathing air (Grade D, Airgas USA, LLC, North Central Region, West Chicago, IL) and 51.6 ± 1% ppmv NO balanced in nitrogen (EPA protocol gas, Praxair, Inc., Danbury, CT) adjusted to a NO concentration of 0.11–1.0 ppmv, relative humidity of 10–70%, and flow rate of 1.5–5.0 $L \cdot min^{-1}$. A UV-A light (XX-15BLB, Ultra-Violet Products, LLC, Upland, CA), directed at the UV-A-transparent optical window located at the top of the photoreactor, activated the photocatalytic properties of the mortar slab. The primary emissions spectrum peak from the light was 365 nm. At the location of the slab surface, the irradiance at 365 nm was measured to be 0.22–1.5 x 10^1 $W \cdot m^{-2}$ using 365 nm UV sensor and radiometer (CX-365 and VLX-3W, Vilber Lourmat, Marne-la-Vallée, France). Except for instances when temperature was investigated as an independent variable, slab temperature was room temperature (approximately 22°C).

As displayed in Figure 3, within the reactor, 25 mm (1 in) wide PMMA spacers secured the slab's position and were set at a height that was either flush with or less than 2 mm below the slab surface. Within the 300 mm long reactor, the gas flowed over the slab through a cross section with a width of 150 mm (6 in) and a height (*H*) of approximately 6 mm (0.25 in). Turbulent airflow over the slab would introduce additional variability in the test. Using the approach detailed in Hüsken et al. (2009), Reynolds number (*Re*) was calculated to be 42.6 using an air kinematic viscosity of 1.54×10^{-5} $m^2 \cdot s^{-1}$ (1.66×10^{-5} $ft^2 \cdot s^{-1}$) and an air flow rate of 3 $L \cdot min^{-1}$ (0.8 $gal \cdot min^{-1}$). The length (L_d) for a parabolic velocity profile in the photoreactor was estimated to be approximately 27.1 mm (1.1 in) by the following equation: $L_d = 0.1 \cdot Re \cdot H$. The estimated length was slightly longer than the length of the PMMA spacers, which indicates that approximately 1.1% of the slab surface did not have a fully developed parabolic velocity profile. At 3 $L \cdot min^{-1}$, theoretical retention time of the test gas within the photoreactor was estimated to be 38 s. Theoretical retention time of the test gas in the volume above the slab at 3 $L \cdot min^{-1}$ was estimated to be 2.7 s.

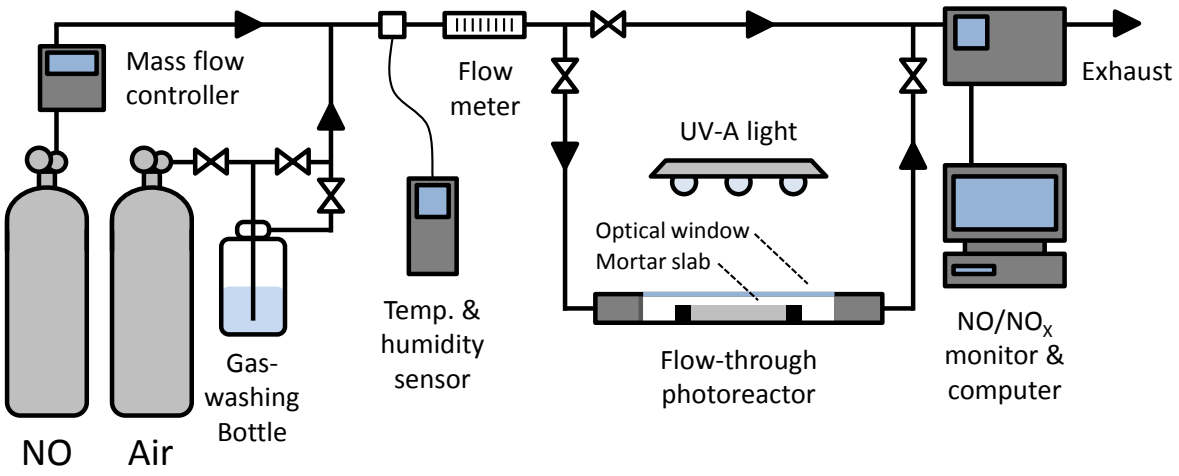

Figure 2. Diagram of experimental apparatus (partially adapted from Ballari et al., 2011).

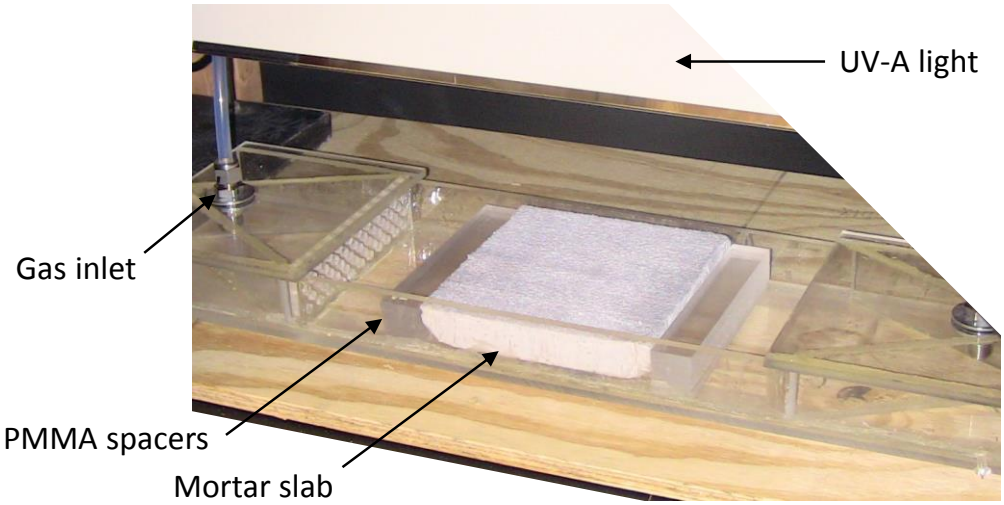

Figure 3. Photograph of photoreactor and mortar slab (optical window removed to facilitate viewing).

A NO/NO_X monitor, (Model 410 Nitric Oxide Monitor and Model 401 NO_2 Converter, 2B Technologies, Inc., Boulder, CO), completed the experimental apparatus. The monitor recorded the gas concentrations at 10 s intervals and was set to measure either NO or NO_X. Unlike chemiluminescence instruments, which detect the light produced when NO reacts with ozone (O_3), the Model 410 measures the change in UV absorbance at 254 nm when O_3 is consumed upon reaction with NO. UV absorbance is an absolute method; therefore, the analyzer requires calibration annually to correct for non-linearity that exists in the photodiode response and associated electronics.

2.3. Operational Procedure

Operation of the experimental apparatus was divided into two phases: parameter setting and testing. While in the parameter setting phase, the test gas flowed through the photoreactor; however, the slab was not irradiated by UV light. This phase was used to set airflow rate, relative humidity, and pollutant concentration and lasted for approximately 10 minutes. After adjusting parameters to desired values, gas flow was maintained through the photoreactor for a period sufficient to reach steady-state conditions.

153 The testing period comprised two steps during which the UV light was turned off and on and
154 concentrations of NO and NO_X were measured. Figure 4 illustrates the UV on and off measurement cycle.
155 Time to complete this cycle was limited to 60 minutes to minimize the possible influence of slab
156 degeneration (e.g., due to the adsorption of reaction products) on collected data. Of note, a gap occurred
157 between measurement of UV light on and off segments. The change in concentration that occurred when
158 the light was turned on or off was not instantaneous. The period between measurements permitted time
159 for concentration stabilization after each parameter change. In some instances, the time gap was not
160 sufficient for concentration stabilization. When analyzing the data strings, these values were identified
161 and removed. The study also did not evaluate adsorption of NO that could occur on the slab or on other
162 surfaces within the photoreactor; rather, in similarity to other studies, this research focused on NO
163 removal that occurred as result of irradiance by UV light (Ballari et al., 2011, Hüsken et al. 2009).

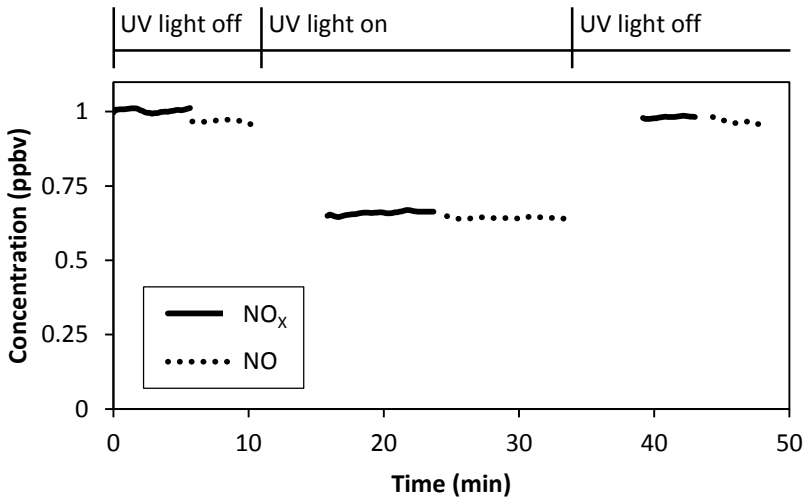

164

165 **Figure 4. Typical NO/NO_X monitor data from testing procedure.**

166 An alternative approach to test for photocatalytic oxidation is to measure NO concentration as the
167 test gas first flows through a bypass line and then is diverted to flow through the photoreactor. With this
168 approach a portion of the decrease in concentration that occurs as the gas flows through the photoreactor
169 could be due to adsorption on the slab and dilution by air leakage. Measuring the difference in

concentration between UV-off and -on periods avoided these error sources and limits the source for a change concentration to photo-oxidation and photo-dissociation. To evaluate whether photo-dissociation occurred within the photoreactor, the researchers also evaluated a slab that was not manufactured with photocatalytic cement (see Control in Table 1). A two-tailed *t*-test, assuming unequal variances, did not find evidence of a significant difference between average UV-off and UV-on NO concentration at 90% confidence (t=3.019, df = 4, p = 0.039).

2.4. Variable Control and Measurement for Completed Tests

To evaluate the objectives listed above, the study collected data on the NO oxidation rates of photocatalytic mortar slabs under varied environmental conditions. In some cases, NO_X oxidation rates were also collected. The following environmental variables were considered: NO concentration ($C_{UV\ off}$), irradiance (*Irrad.*), test gas flow rate (Q), relative humidity (RH), decrease in slab moisture, and slab temperature (*Temp*). Table 1 presents values of these variables for the tests of NO concentration, irradiance, test gas flow rate, relative humidity, and slab temperature. For these tests, at the initial measurement (Test ID 0), all variables were set at the values specified by ISO 22197-1:2007(E) (i.e., $C_{UV\ off}$ = 1.0 ppmv, *Irrad.* = 10 $W \cdot m^{-2}$, Q = 3.0 $L \cdot min^{-1}$, RH = 50%). In subsequent tests, each independent variable was decreased or increased from the ISO-specified values in order to evaluate the change in NO and NO_X oxidation. To facilitate comparison to other published work, selected values of these variables were similar to values reported in said studies.

188

Table 1. Environmental conditions and results of tests completed.

		Environmental conditions									Results					
Test #	Slab ID	Description	$C_{UV\ off}$ (ppmv)				Irrad. ($W \cdot m^{-2} \times 10^{1}$)	Q ($L \cdot min^{-1}$)	RH (%)	Slab temp. (°C)	$C_{UV\ on}$ (ppmv)				Oxidation rate ($nmol \cdot m^{-2} \cdot s^{-1}$)	
			NO_X		NO						NO_X		NO		NO_X	NO
			x̄	s	x̄	s					x̄	s	x̄	s		
0		Control			1.1	0.00067	1.0	3.0	50	22[i]			1.1	0.0033		0.36
0	1	Initial	1.0	0.0039	1.0	0.0046	1.0	3.0	50	22[i]	0.71	0.0022	0.64	0.00054	34	42
1	1	Δ conc.	0.12	0.014	0.11	0.011	1.0	3.0	50	22[i]	0.068	0.00062	0.043	0.0019	6.5	9.8
2	1	Δ conc.	0.31	0.013	0.30	0.010	1.0	3.0	50	22[i]	0.19	0.00055	0.15	0.00063	15	19
3	2	Δ irrad.	1.0	0.0030	1.0	0.0036	0.22	3.0	50	22[i]	0.93	0.00035	0.89	0.00030	7.5	10
4	2	Δ irrad.	1.0	0.0054	1.0	0.012	0.40	3.0	50	22[i]	0.88	0.00030	0.83	0.00031	11	15
5	2	Δ irrad.	1.0	0.0015	1.0	0.0029	0.70	3.0	50	22[i]	0.88	0.0011	0.82	0.0015	15	20
6	2	Δ irrad.	1.0	0.0060	1.0	0.0034	1.0	3.0	50	22[i]	0.86	0.0012	0.79	0.00041	17	25
7	2	Δ irrad.	1.0	0.0049	1.0	0.0051	1.5	3.0	50	22[i]	0.76	0.0013	0.69	0.0012	27	34
8	1	Δ Q	1.0	0.020	1.0	0.016	1.0	1.5	50	22[i]	0.58	0.0018	0.51	0.00055	28	33
9	1	Δ Q	1.0	0.0075	1.0	0.0068	1.0	5.0	50	22[i]	0.84	0.0036	0.79	0.00055	27	35
10	1	Δ RH	1.0	0.0054	1.0	0.011	1.0	3.0	10	22[i]	0.55	0.0021	0.50	0.0017	59	64
11	1	Δ RH	1.0	0.0037	1.0	0.0041	1.0	3.0	20	22[i]	0.59	0.0024	0.52	0.00083	52	61
12	1	Δ RH	1.0	0.0034	1.0	0.0044	1.0	3.0	70	22[i]	0.80	0.0025	0.73	0.00069	23	28
13	3	Δ temp.			1.0	0.0003	1.0	3.0	20	55			0.72	0.0041		30
14	3	Δ temp.			1.0	0.0024	1.0	3.0	20	49			0.72	0.0049		31
15	3	Δ temp.			1.0	0.0005	1.0	3.0	20	44			0.78	0.0060		26
16	3	Δ temp.			1.0	0.0010	1.0	3.0	20	39			0.70	0.0022		25
17	3	Δ temp.			1.0	0.00073	1.0	3.0	20	36			0.69	0.0029		27
18	3	Δ temp.			0.92	0.0017	1.0	3.0	20	34			0.70	0.0016		22
19	3	Δ temp.			0.92	0.0013	1.0	3.0	20	32			0.73	0.0054		18
20	3	Δ temp.			0.92	0.0077	1.0	3.0	20	19			0.73	0.0079		19
21	3	Δ temp.			0.88	0.0019	1.0	3.0	20	21			0.71	0.0013		17
22	3	Δ temp.			0.94	0.0018	1.0	3.0	20	22			0.78	0.0022		16
23	3	Δ temp.			1.0	0.0018	1.0	3.0	20	7.1			0.85	0.0041		13
24	3	Δ temp.			1.0	0.0013	1.0	3.0	20	13			0.81	0.0021		16
25	3	Δ temp.			1.0	0.0011	1.0	3.0	20	15			0.81	0.0042		14

[i] slab temperature not measured during test; room temperature assumed

189

190 *2.4.1. NO concentration, irradiance, test gas flow rate, and relative humidity*

191 Needle valves and a mass flow controller permitted control of NO concentration, test gas flow rate,
192 and relative humidity. To control irradiance the distance between the UV light and photoreactor optical
193 window was varied until the target value was observed on the radiometer at the height of the slab surface.

194 *2.4.2. Slab temperature*

195 Prior to evaluation in the photoreactor, a pre-cleaned slab (procedure in Section 2.1) was brought to
196 an initial temperature that was either above or below room temperature. To obtain this initial
197 temperature, a slab was placed in either an oven (60°C) or a refrigerator (2-4°C) for a period of 2 h. After
198 removal from the oven or refrigerator, the slab was immediately loaded into the photoreactor. An infrared
199 thermometer (15-077-966, Thermo Fisher Scientific, Waltham, MA) recorded temperature at 5 points on
200 the slab surface (the slab center and the center of each quadrant) immediately prior to and after
201 photoreactor evaluation. If slab temperature was greater than room temperature, photocatalytic
202 evaluation began after temperature recording. When slab temperature is less than the test gas
203 temperature (22°C), the possibility of water vapor condensation—which would blind photocatalytically
204 active sties—must be considered because this condensation would falsely indicate reduced photo-
205 activity. This error can be minimized by ensuring that the lowest slab temperature is substantially above
206 the dew point temperature of the test gas. To create a substantial difference between temperatures, the
207 researchers selected a 20% relative humidity for the test gas (dew point = -2°C). As a result, even if the
208 test gas air cooled 5°C as it flowed over a cool slab, relative humidity would only increase to 60% and
209 saturation of the test gas would not occur. To further minimize this potential error, the researchers
210 attempted to evaporate condensed water by using valves to reduce the test gas relative humidity to 0%
211 for a 10 minute period. Following this period, the UV light was turned on, relative humidity was increased
212 to the target value (20%), and photocatalytic evaluation began. The possibility exists that the effort to

avoid error by water condensation was unsuccessful. This possibility was evaluated by comparing the slope of the NO oxidation rate versus temperature line for observations below and above 22°C (Section 3.1.6). It must also be noted, that in this portion of the study, the researchers sought to ensure that water vapor density remained constant throughout the tests, rather than relative humidity. To achieve this goal, relative humidity was set in reference to the test gas temperature, which remained constant, rather than the variable slab temperature.

Additional NO oxidation rate evaluations were completed in succession as the slab temperature increased or decreased. Three sets of successive tests were recorded at the following temperature classifications: hot (32–55°C, Test IDs 13–19), warm (19–22°C, Test IDs 20–22), and cool (7.1–15°C, Test IDs 23–25) as shown in Table 1. Conducting successive tests could lead to a decrease in reactivity over time; therefore, the testing period was reduced such that the total testing time for the hot, warm, and cool classifications was 90, 40, and 40 minutes, respectively. Slab temperature was not measured at the midpoint of each test; instead, this value was estimated. The temperature and time data collected during the hot (n = 40), warm (n = 20), and cold (n = 20) sets of successive tests fit power law curves when adjusted for asymptotic values (R^2 > 0.95 for each set). For example, temperature for the hot classification was estimated using the following equation: $T = 5 \times 10^{-5} \cdot [(t + 647)/1440]^{-16.76} + 28$ ($T = temperature\ in\ °C, t = elapsed\ time\ in\ minutes, R^2 = 0.99$). These curves were used to estimate slab temperature at the midpoint of the photoreactor test.

2.4.3. Decrease in slab moisture

To evaluate the effect of a decrease in slab moisture, NO oxidation was periodically evaluated as water content decreased after starting at a saturated state. For these tests, NO concentration was set to 1.0 ppmv, flow rate to 3 L·min^{-1}, relative humidity to 20% and UV-A irradiance to 10 W·m^{-2} at 365 nm. In similarity with the approach used in Section 2.4.2, a constant vapor density was ensured by setting relative

humidity in reference to the test gas temperature. To achieve saturation, a slab was immersed in water for 24 h. To promote a decrease in slab moisture, the slab was placed in a 60°C oven. The slab was periodically removed from this oven in order to measure slab mass and NO oxidation rate. Testing continued for the duration of 48 h. The decrease in slab moisture was presented as a percentage using the mass at the point of saturation and the calculated moisture loss (i.e., the difference in mass at saturation and at the point of photoreactor evaluation).

2.5. Presentation of Results

Other published works present NO removal as a percentage based on the difference between UV-off and -on concentrations of NO. Percent removal data is in part a function of lab setup (e.g., slab dimensions). Presenting results in this manner can lead to misperceptions if, for example, results are not normalized by area. In this research results are presented as the average NO oxidation rate in the reactor volume using the equation given by Minero et al. (2013):

$$NO\ oxidation\ rate = \frac{P}{R \cdot T} \cdot \frac{Q}{A} \cdot C_{UV\ off} \cdot ln\left(\frac{C_{UV\ off}}{C_{UV\ on}}\right) = \left[\frac{nmol}{m^2 \cdot s}\right]$$

where,

$P = atmospheric\ pressure = \ 101.3\ kPa$,

$R = ideal\ gas\ constant = 8.314 \times 10^{-12}\ m^3 \cdot kPa \cdot nmol^{-1} \cdot K^{-1}$,

$T = temperature = [K]$,

$Q = volumetric\ flow\ rate = [m^3/s]$

$A = slab\ surface\ area = 0.023\ m^2$,

$C_{UV\ off} = NO\ concentration\ with\ UV\ light\ off = [ppmv]$, and

$C_{UV\ on} = NO\ concentration\ with\ UV\ light\ on = [ppmv]$.

The recorded test gas temperature was used to calculate oxidation rate for evaluations of NO concentration, irradiance, flow rate, and relative humidity. Due to the low mass flow rate (5.6×10^{-5} kg·s^{-1}) and specific heat of air (1.007 kJ·kg^{-1}·°C^{-1}), evaluations of slab temperature and slab moisture assumed that the test gas temperature was the same as the slab temperature.

3. Results and Discussion

3.1. NO Oxidation Rate for Tests Completed

Table 1 documents the environmental parameters and oxidation rate results of the tests completed for this study. Of note, in each instance the value of NO oxidation rate is greater than that of NO_X oxidation rate. It could be expected that since the test gas supply to the reactor was nearly entirely comprised of NO, then the NO and NO_X removal values would be the same value. The discrepancy arises because NO is not oxidized completely to HNO_3. Rather, a portion of the gas is transformed to NO_2. NO_2 that remained in the gas stream was counted as part of the outlet NO_X concentration. As a result, NO_X removal measured lower than NO removal.

In this study, all slabs were prepared with the same procedure, materials, and proportions but in different batches. Review of Table 1 finds that although Tests IDs 0 and 6 were evaluated at the same environmental conditions, the observed NO oxidation rate differed by 51% from the mean. This difference may be due to several non-obvious factors within the mixing, placement, and curing steps. Prior research also indicated that oxidation rate differences may occur between slab replicates. For example, Hüsken et al. (2009) found that the percent difference of degradation rates for various replicates of photocatalytic pavement materials varied from as low as 0% to as high as 63%. Noting that differences did occur between slab replicates, Figures 5 to 9 plot each independent variable versus NO oxidation rate for a selected slab. To place this study's observations in context, overlaid on these plots are the data reported from previous

research that investigated NO oxidation rates under differing environmental conditions (Ballari et al., 2010; Ballari et al., 2011; Hüsken & Brouwers, 2008; Hüsken et al., 2009; Murata et al., 2000).

3.1.1. Influent NO Concentration

Figure 5 indicates a correlation between inlet NO concentration and NO oxidation rate (R^2 = 0.994) This correlation is also evident in the data from Murata et al. (2000) (R^2 = 0.984 for 0–1.0 ppmv, R^2 = 0.802 for 0–5.0 ppmv), Hüsken and Brouwers (2008) and Hüsken et al. (2009) (R^2 = 0.991), and Ballari et al. (2010) (R^2 = 0.882).

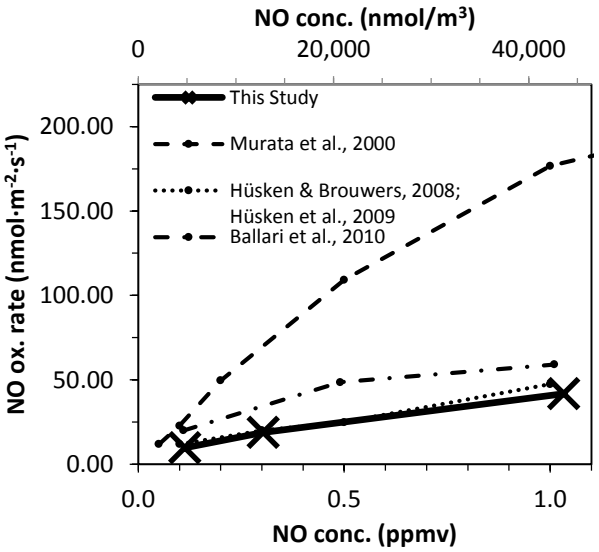

Figure 5. Effect of influent NO concentration on NO oxidation rate.

A correlation between inlet concentration and NO oxidation rate was previously reported by Herrmann (1999). This publication indicated that kinetics follow a Langmuir-Hinshelwood mechanism, under which both reactants adsorb (e.g., NO and •OH) on the surface before a new molecule is formed. For these type of reactions, kinetics typically fell into low-concentration and high-concentration classifications. In the low-concentration classification, oxidation kinetics were first-order; whereas in the high-concentration classification, oxidation kinetics were zero-order. As applied to NO degradation by

photocatalytic pavements, this framework would indicate that, at high concentration, the rate of NO oxidation would remain constant. A constant oxidation rate occurred because a finite number of active sites were available for photocatalytic degradation. Once these sites were occupied, the rate of oxidation did not increase. In contrast, while within the low-concentration classification, the active sites had not yet been filled (Herrmann 1999).

For reactants adsorbed from aqueous phases, Herrmann (1999) indicated that a first-order kinetics apply when concentration is less than 10^{-3} M and zero-order kinetics apply at a concentration greater than 5×10^{-3} M. These divisions have not been established for reactants adsorbed from a gas phase. Except for Ballari et al. (2010), which only had 3 observations, *t*-tests of the data presented in Figure 5 rejected a null hypothesis that slope equaled 0 nmol $m^{-2} \cdot s^{-1} \cdot ppmv^{-1}$ (p = <0.033). Based on this analysis, it is evident that this data falls into first-order oxidation kinetics, indicating that active sites have not been filled. For applications of photocatalytic pavement, a determination of where the breakpoint between first- and zero-order oxidation kinetics occurs is not necessary. Locations where these pavements may be installed can be assumed to have NO_X concentrations near the National Ambient Air Quality Standards (NAAQSs) for NO_2 (i.e., 53 and 100 ppbv) (Primary National Ambient Air Quality Standards for Nitrogen Dioxide: Final Rule, 2010). These values are substantially below the 1.0 ppmv upper limit of the data analyzed; therefore, field applications can also be assumed to be characterized by first-order oxidation kinetics.

In addition to finding evidence that influent NO concentration affects NO oxidation rates, a *t*-test which compared the slope of linear regression lines for the presented data sets found no significant difference between this study's data and the data from Hüsken and Brouwers (2008) and Hüsken et al. (2009) (t = -1.429, df = 3, p = 0.248), and Ballari et al. (2010) (t = -0.515, df = 2, p = 0.658). A similar *t*-test did find that the slope was significantly different than the 0–1.0 ppmv data from Murata et al. (2000) (t = -10.834, df = 4, p = 0.000). Review of Murata et al. (2000)'s writing found that the reactor setup was not

markedly different that that of the authors'; therefore, material chacateristics are also likely to influence the activity of photocatalytic pavements. More broadly, it can be concluded that because these slopes are significantly different, a generalized assumption of the effect of NO concentration on NO oxidation rate cannot be made. Instead, if a photocatalytic material is to be used in the field, it would be wise to complete lab evaluations in order to project levels of oxidation that could be observed in the field.

3.1.2. UV-A Irradiance

Figure 6 indicates a positive correlation between UV-A irradiance and NO oxidation (R^2 = 0.996). This correlation is also evident in the data from Murata et al. (2000) (R^2 = 0.910), Hüsken et al. (2009) (R^2 = 0.940), and Ballari et al. (2011) (R^2 = 0.986). This positive correlation exists because increased UV-A irradiance on a photocatalytic surface increases the rate at which electron holes are created. An increase in the rate of electron-hole generation results in the increased production rate of hydroxyl radicals, which oxidize NO. Multiple publications report that the relationship between irradiance and pollutant oxidation can be divided into two classifications. Although disagreement exists on the value of the division point between classes (10–250 $W \cdot m^{-2}$), the publications note a linear relationship below the division point and a non-linear relationship above this point (Herrmann et al., 2007; Jacoby et al., 1995; Kumar et al., 1995; Lim et al., 2000; Obee & Brown, 1995). Jacoby et al. (1995) explains that under the linear classification, electron holes are filled by reactions with species on the photocatalytic surface (e.g., OH^-) faster than by recombination with excited electrons; in contrast, under the non-linear classification, holes are filled by recombination at a faster rate than by reaction with other species.

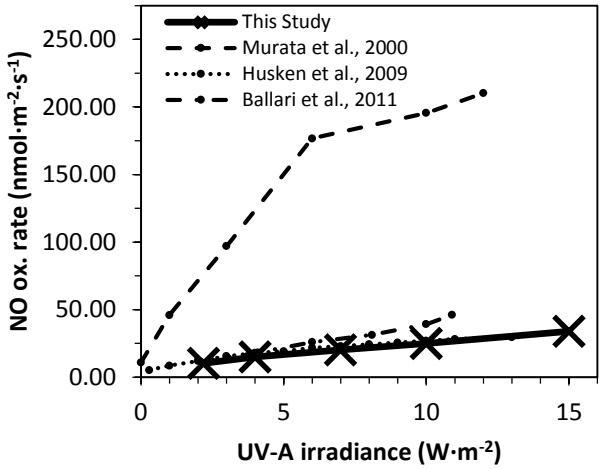

Figure 6. Effect of UV-A irradiance on NO oxidation rate [Ballari et al. (2011) collected data at 0.52 ppmv inlet NO concentration, all other studies used a 1.0 ppmv inlet NO concentration].

As noted above, a linear relationship is apparent when reviewing the data collected in this study (R^2 = 0.996). Comparison of this data with Hüsken et al. (2009) did not find a significant difference in the slope of each data set's linear regression lines (t = -0.403, df = 14, p = 0.693). However, it should be noted that Hüsken et al. (2009) asserted power law relationship between percent NO removal and irradiance ($y = 8.583x^{0.431}$, R^2 = 0.998) and concluded that linear behavior was limited to observations above 4 W·m^{-2}. Linear behavior is also apparent in Ballari et al. (2011) (R^2 = 0.986), but comparison of slopes did find a significant difference (t = -8.462, df = 7, p = 0.000). In contrast, the data from Murata et al. (2000) appears non-linear (R^2 = 0.910 for linear regression). Furthermore, a t-test comparing the slope of linear regression lines between this data set and the authors' found a significant difference (t = -5.672, df = 7, p = 0.001). In similarity with the conclusion reached in Section 3.1.1, this difference indicates that lab evaluation of a specific material selected for field application is warranted in order to assess its NO oxidation potential.

As reported by Grant and Slusser (2005), mean daytime UV-A irradiance ranged from 10.5 to 22.3 W·m^{-2} for the most northern and southern locations (Fairbanks, Alaska, latitude 65.1°N and Homestead, FL, latitude 25.4°N, respectively) according to the United States Department of Agriculture (USDA) climate

monitoring network. In addition to knowledge of the mean UV-A irradiance, application of photocatalytic pavement also requires knowledge on the change in irradiance during daylight hours. This knowledge is needed because in urban areas NO_X ambient concentration reportedly follows a diurnal pattern associated with traffic. Urban background monitoring in London, UK, found that NO_2 peaks both in early morning and late afternoon and NO, which oxidizes quickly to NO_2 during daylight hours, peaks in early morning (Bigi & Harrison, 2010). At these peaks, irradiance values are substantially lower than the mean daytime value. For example, at the 40^{th} parallel north, which roughly runs through the center of the United States, the difference between the typical mid-summer peak UV radiation and the radiation 4 hours earlier in the day is more than 70% (Long et al., 1996). At present, oxidation rates at these low irradiance values are quite low. To be effective at peak pollution hours, the ongoing efforts by other researchers to enhance TiO_2's photo-induced reactivity must be incorporated into new formulations of photocatalytic pavements.

3.1.3. Flow Rate

A model utility test on the data collected in this study (presented in Figure 7) did not reject a null hypothesis that slope equaled 0 $nmol \cdot m^{-2} \cdot s^{-1} \cdot °C^{-1}$ ($t = 0.118$, $df = 2$, $p = 0.925$), and therefore did not provide evidence of a correlation between flow rate and NO oxidation rate. The same conclusion was found with analysis of data from Hüsken and Brouwers (2008) and Hüsken et al. (2009) ($t = 0.631$, $df = 2$, $p = 0.642$). The independence of oxidation rate and flow rate aligns with the overall approach used by Hunger et. al (2010) to model the oxidation of NO on photocatalytic concrete surfaces. Using a Langmuir-Hinshelwood model and data collected with a photoreactor, Hunger et. al (2010) established that it is the conversion of adsorbed species that limits the reaction rate, rather than mass transfer from the test gas to the sample surface.

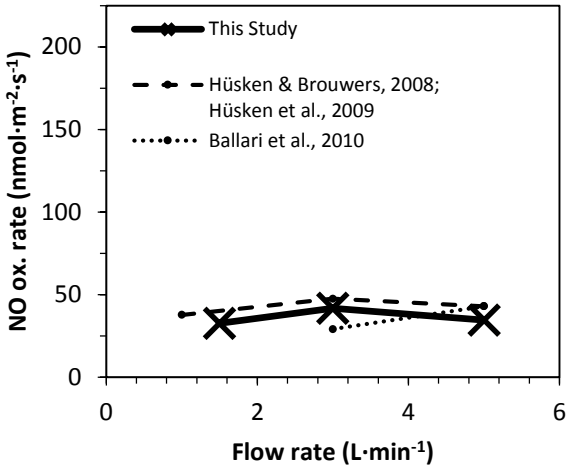

374

375 **Figure 7. Effect of flow rate on NO oxidation rate.**

376 Results, presented in the form of percent NO removal, were determined to be 51, 37, and 21% for
377 flow rates of 1.5, 3, and 5 $L \cdot min^{-1}$, respectively. Using these units, a negative relationship was evident
378 between flow rate and percent removal (t = -27.718, df = 2, p = 0.023). This relationship was also
379 documented by other researchers (Ballari et al., 2010; Dylla et al., 2010; Hüsken & Brouwers, 2008; Hüsken
380 et al., 2009). These studies suggested that percent NO removal from a specific volume of test gas increases
381 proportionally to the residence time over a photocatalytic surface because more time exists for pollutants
382 to absorb and be oxidized at active sites. Overall, the lack of a correlation between flow rate and NO
383 oxidation rate could simplify modeling efforts as stakeholders consider field applications. However, given
384 the wide array of variables that need to be considered, this modeling effort will be challenging and is likely
385 to have a high degree of uncertainty.

386 *3.1.4. Relative Humidity*

387 Figure 8 indicates a negative correlation between relative humidity and NO oxidation rate for the
388 mortar slabs (created with cement that contains TiO_2) used in this study (R^2 = 0.996, t = -22.257, df = 3, p
389 = 0.002). This correlation was also found in the study by Murata et al. (2000) (t = -4.307, df = 5, p = 0.013)
390 and Hüsken and Brouwers (2008) and Hüsken et al. (2009) (t = -22.408, df = 7, p = 0.000). Photocatalytic

391 degradation of NO by pavement containing titanium dioxide occurs when NO is oxidized by •OH (Figure
392 1). These •OH are generated by oxidation of an OH^- by an electron hole. Current understanding proposes
393 that water adsorbed on the slab serves as the source for OH^-. Intuition would thereby suggest that
394 increased humidity would result in an increased rate of NO oxidation. By observation, the opposite has
395 been found to be true. In addition to photocatalytic properties, materials containing TiO_2 also exhibit
396 photo-induced superhydrophilicity (i.e., water on the surface has a contact angle of nearly 0°) (Fujishima
397 et al., 2008). Adsorbed water vapor disperses over the surface, blinding photocatalytically active sites
398 (Beeldens, 2007).

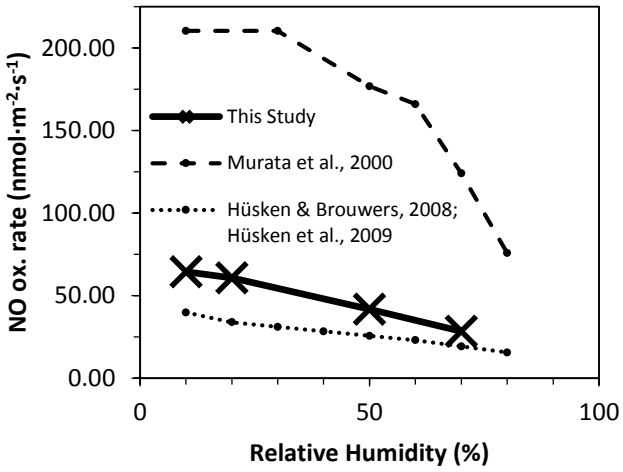

399

400 **Figure 8. Effect of relative humidity on NO oxidation rate.**

401 Although a negative correlation was found in each data set displayed in Figure 8, both data values and
402 relationships differed. A null hypothesis that the difference in slopes of regression lines was 0 (i.e., H_O: B_1
403 – B_2 = 0) was used to compare this study's data to the data obtained by other researchers. This evaluation
404 found a significant difference in slope between this study and both Murata et al. (2000) (t = 2.859, df = 6,
405 p = 0.029) and Hüsken and Brouwers (2008) and Hüsken et al. (2009) (t = -9.378, df = 8, p = 0.000).
406 Evaluation of the y-intercept found a significant difference between this study and both Murata et al.
407 (2000) (t = -423.737, df = 6, p = 0.000) and Hüsken and Brouwers (2008) and Hüsken et al. (2009) (t =

978.105, *df* = 8, *p* = 0.000). This evaluation provides further evidence of the complexity of photocatalytic pavement materials. As concluded in previous sections, the researchers recommend that individual materials undergo a thorough evaluation prior to field evaluation.

The observed negative correlation that occurs as a result of water's blinding effect could limit the effectiveness of photocatalytic pavement in humid regions. Based on 2006–2008 data, the five counties with the highest ambient NO_2 concentration in the form of the 2010-promulgated NO_2 standard for counties within the United States are as follows: Cook, IL, San Diego, CA, Los Angeles, CA, Erie, NY, and Denver, CO (USEPA, 2010a). With the exception of Denver County, each of the listed counties frequently experiences high humidity conditions. As displayed in Figure 8, the NO oxidation rate at high humidity is substantially diminished. Unless photocatalytic pavements can be modified to lessen their sensitivity to changes in relative humidity, effective application in these polluted areas will be difficult.

3.1.5. Decrease in Slab Moisture

Figure 9 presents data obtained from a slab that was periodically removed from a 60°C oven and evaluated in the photoreactor as internal moisture decreased from a saturated state. For a decrease in moisture of 0–2% of saturated mass, a positive correlation is apparent (R^2 = 0.822) and a 0 slope null hypothesis was rejected (*t* = 4.310, *df* = 5, *p* = 0.013). Conversely, for a decrease in slab moisture greater than 2% of saturated mass, a negative correlation is apparent (R^2 = 0.985) and a 0 slope null hypothesis was rejected (*t* = -14.152, *df* = 5, *p* = 0.001). These observations can be explained as follows: between 0 and 2% decrease in moisture, as water is evaporated from the slab it no longer blinds active sites and the NO oxidation rate increases. This explanation is similar to the explanation for the correlation between relative humidity and NO oxidation rates. For a decrease in moisture above 2% the rate of NO oxidation appears to be limited because water contained within the slab is not available as a source for $^{\bullet}OH$. While the primary purpose of these results is to indicate that slab moisture influences NO oxidation rate, it is

worth noting that these tests occurred at an average slab temperature of approximately 50°C. Data presented in Section 3.1.6 indicates that this elevated slab temperature increased reactivity by 60% in comparison to slabs at 22°C.

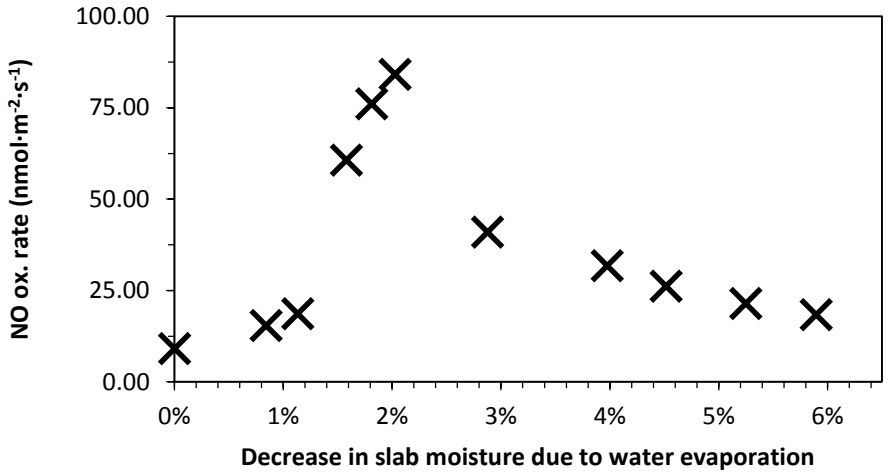

Figure 9. Effect of decrease in slab moisture due to water evaporation on NO oxidation rate (photoreactor vapor density held constant).

In this study, the peak NO oxidation rate was observed at 2% decrease in slab moisture. Under field condition a different peak would be observed. This difference would arise because water content varies throughout the depth of a concrete pavement; therefore, the decrease in moisture at the pavement surface would differ from the decrease in moisture throughout the entire slab. Overall, the findings presented in Figure 9 complicate recommendations for field application of TiO_2-containing pavements. On the basis of relative humidity, areas with sustained periods of low humidity would be recommended for application. It would be assumed that mitigation of NO pollution would continue as long as relative humidity remained low. However, sustained low humidity would also cause evaporation of water contained in the pores of the slab. Based on the data presented, a photocatalytic concrete pavement could be expected to remove NO initially; however, over time NO oxidation would decrease and the benefits would be lost. If TiO_2-containing pavement is to be applied in the field to mitigate NO pollution,

this complicating factor requires further investigation and methods to maintain moisture in the pavement may need to be developed.

3.1.6. Slab Temperature

Figure 10 displays the effect of temperature on NO oxidation rate on axes of NO oxidation rate versus temperature (Figure 10a) and $ln(NO\ oxidation\ rate)$ versus the inverse of temperature (Figure 10b). Linear regression of this data found a R^2 value of 0.880. A model utility test rejected a null hypothesis that slope equaled 0 nmol·m^{-2}·s^{-1}·°C^{-1} with confidence in excess of 99.99% (t = 8.963, df = 12). As noted in Section 2.4.2, tests which occurred at slab temperatures below 22°C presented the possibility of error due to water condensation. Linear regression of data points above 22°C found a slope of 0.459 nmol·$^{-2}$·s^{-1}·°C^{-1} (R^2 = 0.725, n = 7); for data points below 22°C the slope was 0.252 nmol·m^{-2}·s^{-1} °C^{-1} (R^2 = 0.417, n = 6). A pooled-variance t-test of a null hypothesis that the difference between these two slopes was 0 (i.e., H_O: $B_1 - B_2 = 0$) indicated that the slopes were not significantly different (t = 0.967, df = 9, p = 0.359). Although the values of the slopes differ, the data collected did not support a claim that this difference was significant.

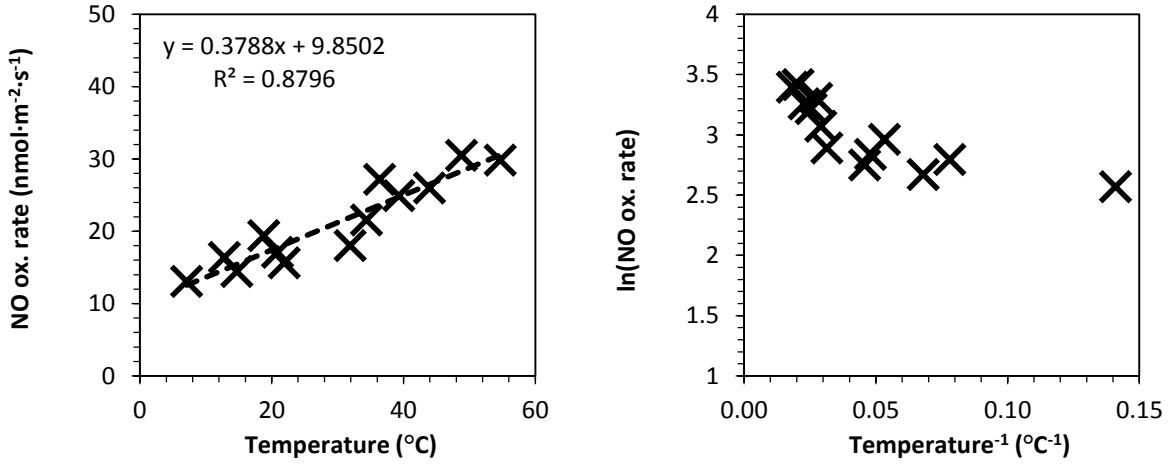

a. **b.**

Figure 10. Effect of temperature on NO oxidation rate.

The effect of temperature on NO oxidation rates has not been studied in previous photoreactor studies; therefore, comparison with other data sets was not possible. Other photocatayltic pavement studies that do make statements in regard to the impact of temperature on oxidation rates are often vague. In most instances these studies assert that the oxidation rate increases with an increase in temperature (Beeldens et al., 2011) and that only large differences in temperature (i.e., summer vs. winter) are significant (Dylla et al., 2011). In addition to being vague, the literature also is contradictory and one source reported a decrease in oxidation rate with increased temperature (Chen & Chu, 2011). One aqueous photocatalysis publication, Herrmann (1999), does provide useful insight for this study. It stated that in the range of 20–80°C, activation energy was negligible and was not a rate limiting step. Furthermore, at temperatures below 0°C, the apparent activation energy of the photocatalyst increased leading to a decrease in oxidation rate.

The Arrhenius equation offers an empirical relationship between a reaction rate constant (k), temperature (T), pre-exponential factor (A), activation energy (E_a), and the universal gas constant (R):

$$k = A \cdot e^{\frac{-E_a}{R \cdot T}}$$

Using log properties, this equation can also be expressed as follows:

$$\ln k = \frac{-E_a}{R}\left(\frac{1}{T}\right) + \ln A$$

When graphed on axes of $ln(NO\ oxidation\ rate)$ and the inverse of temperature ($1/T$), reactions that follow the Arrhenius equation exhibit a linear relationship. Figure 10b does not display this type of relationship. Overall, while the information discussed in this section partially explains the observations; it would appear that given the complexity of photocatalytic pavement materials, other factors also influenced the reported observations.

4. Conclusions

Photocatalytic pavements offer a novel technological option to mitigate NO_X pollution. In order for these pavements to be adopted by potential stakeholders, information is needed that documents the NO oxidation rate under varied environmental conditions. A positive correlation was observed between NO oxidation rate and influent NO concentration. Comparison of this study with Hüsken and Brouwers (2008), Hüsken et al. (2009) and Ballari et al. (2010), who also studied cementitious photocatalytic pavements, found no significant difference in the slope of regression lines through this data. However, a significant difference in slope was observed in comparison with Murata et al. (2000). A positive correlation was also observed between NO oxidation rates and UV-A irradiance (R^2 = 0.996). Comparison of this study with Hüsken et al. (2009) found no significant difference in the slope of regression lines through this data. A significant difference in slope was observed in comparison with Murata et al. (2000). A correlation was not observed between NO oxidation rates and flow rate. This same conclusion was reached with analysis of data from Hüsken and Brouwers (2008) and Hüsken et al. (2009). A negative correlation was observed between NO oxidation rate and relative humidity. In contrast with evaluations for UV-A irradiance and NO concentration, no significant difference was found with comparison of this study to Murata et al. (2000). A significant difference in slope was observed between this study and Hüsken and Brouwers (2008) and Hüsken et al. (2009). Decrease in slab moisture, a variable not investigated in prior work, was found to affect NO oxidation rates. At losses of 0–2% of saturated mass, a positive correlation was observed; whereas, at losses greater that 2% a negative correlation was observed. A positive correlation was documented for slab temperature. This finding contrasts previous assertions which considered this variable insignificant.

Overall, it can be concluded that photocatalytic mortar slabs manufactured with TX Active pavement are highly sensitive to changes in environmental variables. NO oxidation rates observed in this study ranged from 9.8–64 $nmol \cdot m^{-2} \cdot s^{-1}$. Furthermore, significant differences were found by comparison to other

studies. Therefore, if a potential stakeholder is considering use of this technology to mitigate NO_X emissions, careful preliminary work should be undertaken to both evaluate the environmental conditions of the test site and the properties of the selected photocatalytic material.

5. Acknowledgments

The authors wish to thank the National Concrete Pavement Technology Center, the United States Department of Transportation *(grant number removed to ensure blind review)*, Essroc Italcementi Group, and Lehigh Hanson, Inc. for providing funding to pursue this study. The authors also thank H. Bai and L. Y. Ong for their role in data collection and analysis.

6. References

Ballari, M. M., Hunger, M., Hüsken, G., & Brouwers, H. J. H. (2010). NOx photocatalytic degradation employing concrete pavement containing titanium dioxide. *Applied Catalysis B-Environmental, 95*(3-4), 245-254. doi: 10.1016/j.apcatb.2010.01.002

Ballari, M. M., Yu, Q. L., & Brouwers, H. J. H. (2011). Experimental study of the NO and NO2 degradation by photocatalytically active concrete. *Catalysis Today, 161*(1), 175-180. doi: 10.1016/j.cattod.2010.09.028

Beeldens, A. (2007, October 8-9). *Air Purification by Road Materials: Results of the Test Project in Antwerp.* Paper presented at the International RILEM Symposium on Photocatalysis, Environment and Construction Materials - TDP 2007, Florence, Italy.

Beeldens, A., Cassar, L., & Murata, Y. (2011). Applications of TiO2 Photocatalysis for Air Purification In Y. Ohama & D. Van Gemert (Eds.), *Application of titanium Dioxide Photocatalysis to Construction Materials* (1st ed.): Springer.

Bigi, A., & Harrison, R. M. (2010). Analysis of the air pollution climate at a central urban background site. *Atmospheric Environment, 44*(16), 2004-2012. doi: 10.1016/j.atmosenv.2010.02.028

Brauer, M., Hoek, G., Van Vliet, P., Meliefste, K., Fischer, P. H., Wijga, A., . . . Brunekreef, B. (2002). Air pollution from traffic and the development of respiratory infections and asthmatic and allergic symptoms in children. *American Journal of Respiratory and Critical Care Medicine, 166*(8), 1092-1098. doi: DOI 10.1164/rccm.200108-007OC

Brunekreef, B., Janssen, N. A. H., deHartog, J., Harssema, H., Knape, M., & vanVliet, P. (1997). Air pollution from truck traffic and lung function in children living near motorways. *Epidemiology, 8*(3), 298-303.

Chen, M., & Chu, J. W. (2011). NO(x) photocatalytic degradation on active concrete road surface - from experiment to real-scale application. [Article]. *Journal of Cleaner Production, 19*(11), 1266-1272. doi: 10.1016/j.jclepro.2011.03.001

Clean Air Act, 42 U.S.C. § 7401 et seq. (2008).

Dylla, H., Hassan, M. M., Mohammad, L. N., Rupnow, T., & Wright, E. (2010). Evaluation of Environmental Effectiveness of Titanium Dioxide Photocatalyst Coating for Concrete Pavement. *Transportation Research Record: Journal of the Transportation Research Board, 2164*(-1), 46-51. doi: 10.3141/2164-06

Dylla, H., Hassan, M. M., Schmitt, M., Rupnow, T., & Mohammad, L. N. (2011). Laboratory Investigation of the Effect of Mixed Nitrogen Dioxide and Nitrogen Oxide Gases on Titanium Dioxide Photocatalytic Efficiency in Concrete Pavements. *Journal of Materials in Civil Engineering, 23*(7), 1087-1093. doi: 10.1061/(asce)mt.1943-5533.0000248

Finkelstein, M. M., Jerrett, M., & Sears, M. R. (2004). Traffic air pollution and mortality rate advancement periods. *American Journal of Epidemiology, 160*(2), 173-177. doi: Doi 10.1093/Aje/Kwh181

Fujishima, A., Zhang, X. T., & Tryk, D. A. (2008). TiO(2) photocatalysis and related surface phenomena. [Review]. *Surface Science Reports, 63*(12), 515-582. doi: 10.1016/j.surfrep.2008.10.001

Garshick, E., Laden, F., Hart, J. E., & Caron, A. (2003). Residence near a major road and respiratory symptoms in US veterans. *Epidemiology, 14*(6), 728-736. doi: DOI 10.1097/01.ede.0000082045.50073.66

Grant, R. H., & Slusser, J. R. (2005). Estimation of ultraviolet-A irradiance from measurements of 368-nm spectral irradiance. *Journal of Atmospheric and Oceanic Technology, 22*(12), 1853-1863. doi: 10.1175/jtech1823.1

Herrmann, J. M. (1999). Heterogeneous photocatalysis: fundamentals and applications to the removal of various types of aqueous pollutants. *Catalysis Today, 53*(1), 115-129.

Herrmann, J. M., Péruchon, L., Puzenat, E., & Guillard, C. (2007, October 8-9). *Photocatalysis: from fundamentals to self-cleaning glass applications.* Paper presented at the International RILEM Symposium on Photocatalysis, Environment and Construction Materials - TDP 2007, Florence, Italy.

Herrmann, J. M. (2010). Photocatalysis fundamentals revisited to avoid several misconceptions. *Applied Catalysis B: Environmental, 99*(3), 461-468.

570 Hunger, M., Hüsken, G., & Brouwers, H. (2010). Photocatalytic degradation of air pollutants—From
571 modeling to large scale application. *Cement and Concrete Research, 40*(2), 313-320.

572 Hüsken, G., & Brouwers, H. J. H. (2008, June 16-20). *Air purification by cementitious materials: Evaluation*
573 *of air purifying properties.* Paper presented at the International Conference on Construction and
574 Building Technology, Kuala Lumpur, Malaysia.

575 Hüsken, G., Hunger, M., & Brouwers, H. J. H. (2009). Experimental study of photocatalytic concrete
576 products for air purification. *Building and Environment, 44*(12), 2463-2474. doi: DOI
577 10.1016/j.buildenv.2009.04.010

578 ISO. (2007). Fine ceramics (advanced ceramics, advanced technical ceramics) -- Test method for air-
579 purification performance of semiconducting photocatalytic materials -- Part 1: Removal of nitric
580 oxide (Vol. 22197-1:2007): ISO.

581 Jacoby, W. A., Blake, D. M., Noble, R. D., & Koval, C. A. (1995). KINETICS OF THE OXIDATION OF
582 TRICHLOROETHYLENE IN AIR VIA HETEROGENEOUS PHOTOCATALYSIS. *Journal of Catalysis,*
583 *157*(1), 87-96. doi: 10.1006/jcat.1995.1270

584 Kim, J. J., Smorodinsky, S., Lipsett, M., Singer, B. C., Hodgson, A. T., & Ostro, B. (2004). Traffic-related air
585 pollution near busy roads - The East Bay children's respiratory health study. *American Journal of*
586 *Respiratory and Critical Care Medicine, 170*(5), 520-526. doi: DOI 10.1164/rccm.200403-2810C

587 Kumar, P., Dushenkov, V., Motto, H., & Raskin, I. (1995). PHYTOEXTRACTION - THE USE OF PLANTS TO
588 REMOVE HEAVY-METALS FROM SOILS. *Environmental Science & Technology, 29*(5), 1232-1238.
589 doi: 10.1021/es00005a014

590 Kundu, P. K., & Cohen, I. M. (2010). *Fluid Mechanics*: Elsevier Science.

591 Lim, T. H., Jeong, S. M., Kim, S. D., & Gyenis, J. (2000). Photocatalytic decomposition of NO by TiO2
592 particles. *Journal of Photochemistry and Photobiology a-Chemistry, 134*(3), 209-217. doi:
593 10.1016/s1010-6030(00)00265-3

594 Long, C. S., Miller, A. J., Lee, H. T., Wild, J. D., Przywarty, R. C., & Hufford, D. (1996). Ultraviolet Index
595 Forecasts Issued by the National Weather Service. *Bulletin of the American Meteorological*
596 *Society, 77*(4), 729-748.

597 Minero, C., Bedini, A., & Minella, M. (2013). On the standardization of the photocatalytic gas/solid
598 tests. *International Journal of Chemical Reactor Engineering*, *11*(2), 717-732.

599 Murata, Y., Kamitani, K., & Takeuchi, K. (2000). *Air Purifying Blocks Based on Photocatalysis.* Paper
600 presented at the Japan Interlocking BLock Pavement Engineering Association World Congress
601 2000, Tokyo, Japan.

602 Murata, Y., & Tobinai, K. (2002). Influence of various factors on NOx removal performance of
603 permeable interlocking block based on photocatalysis. *Journal of Structural and Construction*
604 *Engineering(Transactions of AIJ)*(555), 9-15.

605 Obee, T. N., & Brown, R. T. (1995). TIO2 PHOTOCATALYSIS FOR INDOOR AIR APPLICATIONS - EFFECTS OF
606 HUMIDITY AND TRACE CONTAMINANT LEVELS ON THE OXIDATION RATES OF FORMALDEHYDE,
607 TOLUENE, AND 1,3-BUTADIENE. *Environmental Science & Technology, 29*(5), 1223-1231. doi:
608 10.1021/es00005a013

609 Paz, Y. (2010). Application of TiO2 photocatalysis for air treatment: Patents' overview. Applied Catalysis
610 B-Environmental, 99(3-4), 448-460. doi: 10.1016/j.apcatb.2010.05.011

611 Primary National Ambient Air Quality Standards for Nitrogen Dioxide: Final Rule, 75 Fed. Reg. 6474 (2010)
612 (to be codified at 40 C.F.R. pts. 50 and 58).

613 Primary National Ambient Air Quality Standards for Nitrogen Dioxide: Proposed Rule, 75 Fed. Reg. 34404
614 (2009) (to be codified at 40 C.F.R. pts. 50 and 58).

615 Thoma, E. D., Shores, R. C., Isakov, V., & Baldauf, R. W. (2008). Characterization of near-road pollutant
616 gradients using path-integrated optical remote sensing. *Journal of the Air & Waste Management*
617 *Association, 58*(7), 879-890. doi: Doi 10.3155/1047-3289.58.7.879

618 USEPA. (2001). *National Air Quality and Emissions Trends Report, 1999*. (EPA 454/R-01-004). Washington,
619 D.C.

620 USEPA. (2007). *Summary of Current and Historical Light-Duty Vehicle Emission Standards*. Washington,
621 D.C.: Retrieved from http://www.epa.gov/greenvehicles/detailedchart.pdf.

622 USEPA. (2008a). *Average Annual Emissions and Fuel Consumption for Gasoline-Fueled Passenger Cars and*
623 *Light Trucks*. (EPA420-F-08-024). Washington, D.C.: Retrieved from
624 http://www.epa.gov/otaq/consumer/420f08024.pdf.

625 USEPA. (2008b). *Integrated Science Assessment for Oxides of Nitrogen – Health Criteria (Final Report)*.
626 (EPA/600/R-08/071, 2008). Washington, D.C.

627 USEPA. (2010a). *Design Values (Average 1-Hour 98th Percentiles over 3 Years) by County for Nitrogen*
628 *Dioxide* Research Triangle Park, NC: Retrieved from
629 http://www.epa.gov/oaqps001/nitrogenoxides/pdfs/NO2_final_designvalues_0608_Jan22.pdf.

630 USEPA. (2010b). *Final Regulatory Impact Analysis (RIA) for the NO_2 National Ambient Air QUality Standards*
631 *(NAAQS)*. Research Triangle Park, NC: Retrieved from
632 http://www.epa.gov/ttnecas1/regdata/RIAs/FinalNO2RIAfulldocument.pdf.

633 USEPA. (2011, July 6). Nitrogen Dioxide: Health Retrieved September 27, 2011, from
634 http://www.epa.gov/air/nitrogenoxides/health.html

Black and White Versions of Color Figures

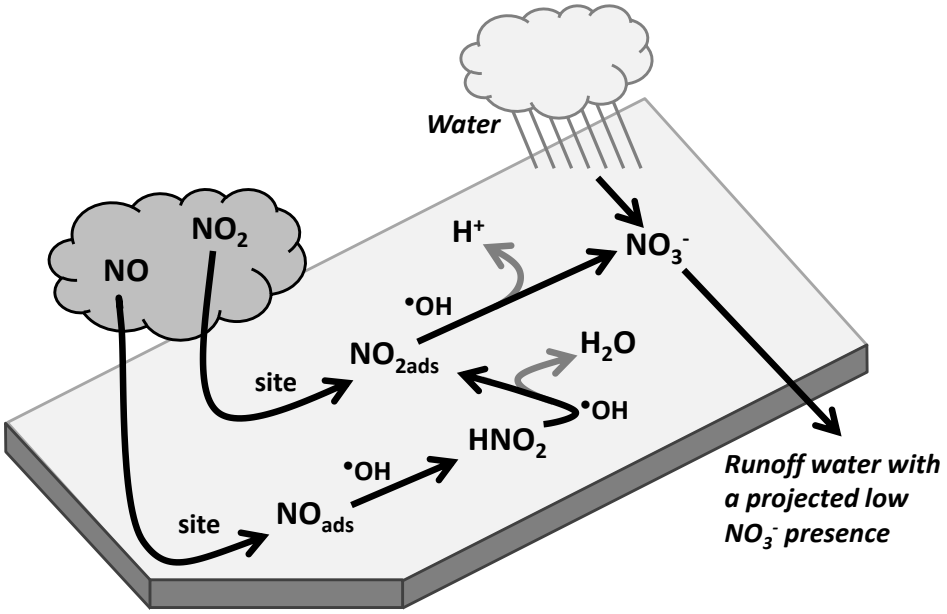

Figure1. Photocatalytic oxidation of NO and NO_2 by pavement containing TiO_2 (partially adapted from Ballari et al., 2011).

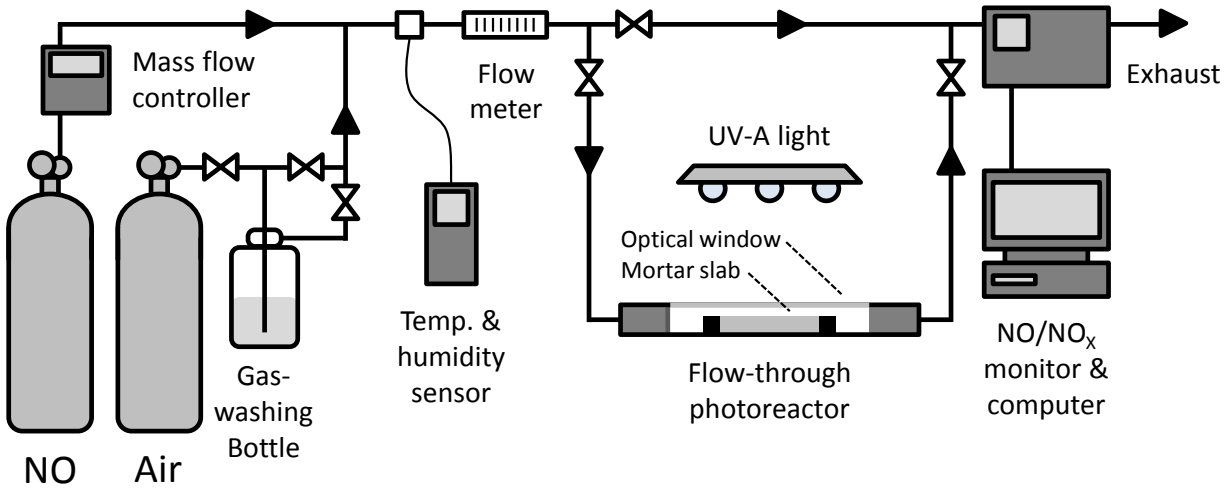

Figure 2. Diagram of experimental apparatus (partially adapted from Ballari et al., 2011).

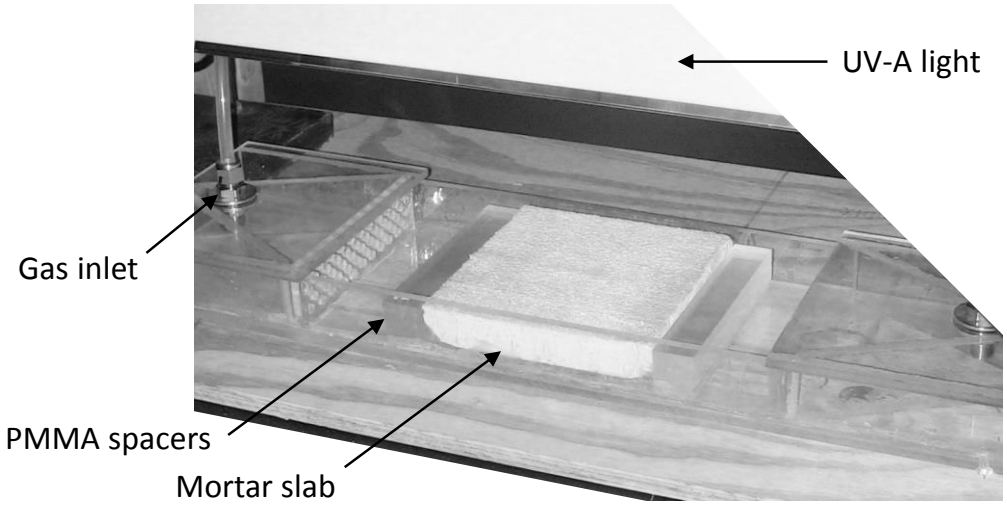

643

644 **Figure 3. Photograph of photoreactor and mortar slab (optical window removed to facilitate viewing).**